Development of sustainable biodegradable lignocellulosic hemp fiber/ polycaprolactone biocomposites for light weight applications

Hom Nath Dhakal, Sikiru Oluwarotimi Ismail, Zhongyi Zhang, Asa Barber, Euan Welsh, Jean-Eudes Maigret, Johnny Beaugrand

PII: S1359-835X(18)30314-2
DOI: https://doi.org/10.1016/j.compositesa.2018.08.005
Reference: JCOMA 5139

To appear in: *Composites: Part A*

Received Date: 29 January 2018
Revised Date: 11 May 2018
Accepted Date: 6 August 2018

Please cite this article as: Nath Dhakal, H., Oluwarotimi Ismail, S., Zhang, Z., Barber, A., Welsh, E., Maigret, J-E., Beaugrand, J., Development of sustainable biodegradable lignocellulosic hemp fiber/ polycaprolactone biocomposites for light weight applications, *Composites: Part A* (2018), doi: https://doi.org/10.1016/j.compositesa.2018.08.005

Development of sustainable biodegradable lignocellulosic hemp fiber/ polycaprolactone biocomposites for light weight applications

Hom Nath Dhakal[a,*], Sikiru Oluwarotimi Ismail[a], Zhongyi Zhang[a], Asa Barber[b], Euan Welsh[a], Jean-Eudes Maigret[c,d], Johnny Beaugrand[c,d]

[a] *Advanced Materials and Manufacturing (AMM) Research Group, University of Portsmouth, School of Engineering, Anglesea Road, Anglesea Building, PO1 3DJ, UK.*

[b] *Bioneer Research Group, University of Portsmouth, School of Engineering, Anglesea Road, Anglesea Building, PO1 3DJ, England, UK.*

[c] *INRA, UMR614 Fractionnement des AgroRessources et Environnement, F-51686 Reims, France.*

[d] *INRA, Research Unit BIA UR1268, Rue Geraudiere, F-44316 Nantes, France*

Corresponding author. Tel: + 44 (0) 23 9284 2582, Fax: + 44 (0) 23 9284 2351.

E-mail: hom.dhakal@port.ac.uk (Hom Nath Dhakal)

ABSTRACT

Biocomposites with poly(ε-caprolactone) (PCL) as matrix and lignocellulosic hemp fiber with varying average aspect ratios (19, 26, 30 and 38) as reinforcement were prepared using twin extrusion process. The influence of fiber aspect ratio on the water absorption behavior and mechanical properties are investigated. The percentage of moisture uptake increased with the aspect ratio, following Fickian behavior. The hemp fiber/PCL biocomposites showed enhanced properties (tensile, flexural and low-velocity impact). The biocomposite with 26 aspect ratio showed the optimal properties, with flexural strength and modulus of 169% and 285% respectively, higher than those of neat PCL. However, a clear reduction on the mechanical properties was observed for water-immersed samples, with reduction in tensile and flexural moduli for the aspect ratio of 26 by 90% and 62%, respectively than those of dry samples. Summarily, the optimal sample provides an eco-friendly alternative to conventional, petroleum-based and non-renewable composites for various applications.

Keywords: A. Polymer-matrix composites (PMCs); B. Fiber/matrix bond; B. Mechanical properties; C. Damage mechanics.

1. Introduction

The growing interest in the use of natural plant fiber as reinforcements in composites is due to their high strength-to-weight ratio, abundant, recoverable and biodegradable nature after the end of their service life. Lignocellulosic fiber comes from renewable resources and they require less energy to produce compared to their conventional counterparts. Cellulose characterised many organic materials, as it supports the advent of green products in materials manufacturing. Its wide applications can be traced to attributes such as versatility, abundancy and compatibility [1]. These properties make natural lignocellulosic fiber attractive reinforcements for polymer matrix composites [2-9]. Comparatively, among some commonly used bast or natural plant fibers such as flax, jute and date palm, hemp fiber has an outstanding physical and mechanical properties, especially in terms of specific tensile strength at break and tensile modulus [4, 10-13].

Lignocellulosic fiber (such as hemp, flax and jute) reinforced composites have been successfully used for light-weight applications in recent years, especially in the automotive and construction industries. This is required in order to reduce an estimated 75% of energy consumption by automobiles, mainly caused by the weight of vehicles [14]. However, significant barriers for structural applications of these composites still exist [15-19]. The full acceptance of natural fiber composites for structural components has been further limited by their inherent complex morphological structure and variation with regard to chemical composition, crystallinity, thermo-mechanical properties, surface roughness and profile.

Conventional polymer matrices such as epoxy, vinyl ester, polyester are attractive for several structural applications as these polymers provide good mechanical properties compared to biodegradable polymers. However, these polymers are non-recyclable and non-biodegradable and as a result they cause serious environmental problems [20,21]. In

this context, the development and use of biodegradable polymers for composites are considered as one of the important strategies for reducing the environmental challenges from the use of petroleum-based and non-biodegradable polymers.

Among the biodegradable matrices such as poly (lactic acid) (PLA), poly (hydroxyalkanoates) (PHA), poly (ε-caprolactone) (PCL) [22,23], PCL has attracted considerable attention as matrix material in manufacturing lignocellulosic biocomposite materials. PCL is one of the relative hydrophobic polymers that are widely used in electronics, packaging, among other day-to-day life applications [24]. Among the biobased matrices, an investigation into the falling weight impact response of jute/methacrylated soybean oil biocomposites under low-velocity impact loading was conducted [15]. Similarly, mechanical performances such as impact strength of PLA-based composite materials have been enhanced when reinforced with addition of carefully designed core-shell and inversed core-shell particles, increased twice than neat PLA matrix [25]. Furthermore, a recent comprehensive review undertaken by Pappu et al. highlighted the industrial potential of renewable and biodegradable banana reinforcements. Their review paper further concluded that banana possesses an excellent mechanical properties such as tensile strength and modulus as well as flexural properties, impact energy, to mention but a few [26]

Additionally, there are several reported works on the development and properties of natural fiber reinforced thermoplastic composites and biodegradable biocomposites for various engineering applications. These properties include, but are not limited to, thermal degradation kinetics [27], mechanical (elastic modulus, tensile strength and modulus), thermo-physical (degradability) and structural [28], among others as well as cyclic and creep [29] and mechanical (3-pont flexural and monotonic tensile) [30]. For examples, the experimental work carried out by Talla et al. [31] highlighted the effects

of hemp fiber reinforcement on the mechanical and structural properties of poly-ethylene terephthalate (PET)-hemp fiber composite samples. They concluded that addition of additives increased the mechanical properties (elastic modulus and strain at break) of the concerned composite samples. Similarly, Talla et al. [32] reported the effect of heating rates on thermostability of the same composite sample. They suggested the possibility of effective melt process of natural fibers/high-melting thermoplastic composites with limited thermal degradation of the reinforcements.

There are not reported works which have systematically and comprehensively investigated the influence of hemp fiber aspect ratio on the mechanical properties and water absorption behavior of lignocellulosic PCL biocomposites.

The objective of the present study was to investigate the reinforcement efficiency of hemp fiber with different fiber aspect ratios on PCL-based biocomposites and compare the influence of aspect ratio on moisture absorption behavior, tensile, flexural and impact properties of hemp fiber/PCL biocomposites.

2. Experimental section

2.1. Materials and methods

Matrix material used was polycaprolactone, which is a semi crystalline polymer and it has a molecular weight of 80000 g/mol. The PCL was used because of its biodegradability and low melting temperature (60 ^{o}C), which is desirable in the compounding of lignocellulosic fiber, such as hemp and it was supplied by Perstop (UK) (Capa© 6800). The hemp (*Cannabis sativa L.)* used was Fedora 17, which was harvested in Aube, France and supplied by FRD©. The aspect ratio plays an important role in the properties such as tensile, flexural and water absorption behaviour of composites. The samples were fabricated alongside with others to determine the influence of aspect ratio on water absorption and mechanical and the performance of a

hemp fiber/polycaprolactone (HF/PCL) biocomposites. This was a combination of a natural hemp fiber and innoxious biodegradable PCL polymer in order to produce a completely biodegradable ‘‘green composite’’, which is environmentally friendly, sustainable and renewable [14,25,33,34].

Fig. 1(a) shows the raw hemp fiber fraction, while Fig. 1(b) is the focus of the Fig. 1(a) where large bundles are dominants. The fiber aspect ratio is the ratio of the mean hemp fiber element length, *l* (µm) to the mean fiber element diameter, *d* (µm) (*l/d*). Therefore, using lengths of 432, 568, 708 and 845 µm and diameters of 22.4, 21.7, 23.6 and 22.5 µm, respectively to produce aspect ratios of 19, 26, 30 and 38, respectively. Figs 1(c) and (d) are illustrations of the extremes average fibers aspect ratio, *l/d* values of 19 and 38 respectively, obtained after processing and after extraction from the PCL matrix. Diameter reduction of the bundles are clearly evidenced, and fragmented bundles and damaged are also observed, as depicted in Fig. 1(c), with the average *l/d* of 19. In Fig. 1(d), the increasing proportion of small bundle diameter or individual fibers is illustrated (average *l/d* of 38).

Figs 1(b) – (d) are from a tabletop microscope scanning electron microscope (TM-1000, Hitachi, Tokyo, Japan). There were no metal coatings of the samples necessary for observing the samples at the magnification presented. The scale bars in Figs. 1(b), (c) and (d) are 100 µm.

2.2 Fabrication of neat PCL and hemp fiber/PCL composite samples

To ensure homogeneity within the fiber, before being later processed, small bundles of scutched bast hemp fibers were first copped manually to length of 1.4 ± 0.34 cm measured by scanner assisted image analysis (Simpalab, Techpap, Grenoble France). The composites were prepared using a laboratory-scale twin screw extrusion (TSE) Clextral BC 21 (Firminy, France). The samples were fabricated using a Clextral BC 21

laboratory-scale twin screw extrusion machine. The extruder had a length of 900 mm and a diameter of 20 mm and two profiles varying in severity were used as reported by Beaugrand and Berzin [35]. Also the hemp and PCL were introduced into the extrusion machine at two different hopper locations. For the average aspect ratio (*l/d)* of 19 and 26, the profile "1" was used, a more severe screw profile than the less severe profile "2" that results in the average of 30 and 38 *l/d*. Once the PCL was melted, the hemp was then added further down in the barrel, resulting in much less severe extrusion conditions than if they were introduced into the hopper zone simultaneously giving the average *l/d* of 19, 26, 30 and 38.

To prevent irregular feeding which usually occurs with long fibres when using either volumetric or gravimetric feeders. In this study, the fibres were therefore fed manually. To do so, during the extrusion the fibres were poured manually at a constant rate into the feeder or the barrel opening having the provision of beakers with 2 g prepared extemporarily.

2.3. Water absorption test

The water absorption tests of hemp fiber/PCL biocomposites were carried out in accordance to the EN ISO 62:1999 [4]. Samples along with neat PCL, (dimension of 70 mm x 70 mm) of four different average aspect ratios: 19, 26, 30 and 38 were dried in a fan-assisted oven at 50 ^{o}C, then cooled to room temperature in a desiccators before weighting them to the nearest 0.1 mg prior to immersion into water bath. This process was repeated until the mass of water immersion specimens were reached constant [4]. Water absorption tests were conducted by immersing the composite samples in a de-ionised water bath at 25 ^{o}C, until the samples reached near saturation. The percentage of water absorption in the neat PCL and hemp fiber/PCL composites was calculated by weight difference between the samples immersed in water and the dry samples.

2.4. Tensile test

Tensile test samples were individually cut from the composite slabs into dumbbell shaped (6 mm thickness, 25 mm gauge length) at room temperature, using water jet cutting, the test was performed on Zwick/Roell Z030 machine. A total of four samples were tested from each type of sample with a crosshead speed of 10 mm/min.

2.5. Flexural test

The PCL and hemp fiber/PCL composites were tested for determining flexural strength and modulus under three-point bending test on Zwik/Roell Z030 machine in accordance BS EN 2746:1998 test method [20]. A total of four samples were tested for each type of the composite samples. The crosshead speed chosen was 2 mm/min.

2.6. Low-velocity impact test

The low-velocity instrumented falling weight impact tests were conducted at room temperature using a Zwick/Rowell HIT230F drop weight impact testing machine. The hemispherical impactor made of steel had a diameter of 19.8 mm with a constant mass of 23.11 Kg (carriage and impactor). For each sample, the weight free fell from a height of 110 mm, generating 25 J, drop velocity of 1.49 m/s, sufficient enough to perforate the samples which were of thickness 6 mm at a size of 70 mm^2 at room temperature. From the aforementioned impact parameters, the piezo load-cell attached in the system calculated important impact characteristics such as load, absorbed energy and actual velocity, which were used to characterise the impact behaviour. For each type of sample, the tests were repeated four times before validation, to ensure test repeatability. The test was conducted in accordance with the British Standard BSEN ISO 6603-2 recommendations [36].

2.7. Scanning electron microscopy

The morphological analysis of the biocomposites was performed by using scanning electron microscopy (SEM) JSM/JEOL 6100 at room temperature. The samples were then placed on stands and coated with gold palladium to enhance the conductivity during imagery.

2.8. X-ray micro computed tomography

Further non-destructive examination of the damaged samples was carried out using X-ray micro computed tomography (simply referred to as X-ray µCT), known as Nikon XT H 225 X-ray µCT scanner.

3. Results and discussion

3.1. Water absorption behavior

Fig. 2 shows average percentage of weight gain as a function of square root of time for PCL and PCL/hemp samples with different aspect ratios immersed in de-ionised water at room temperature (25 ^{o}C). The moisture uptake curves for all hemp fiber/PCL samples with different aspect ratio display three well separated zones. At shorter times, zone 1, ($t<15.5$ hrs^{½}), the kinetics of absorption is very fast. At intermediate times, zone 2, ($t>15.5$-21.9 hrs^{½}) the kinetics of moisture absorption is slow, whereas at longer times, zone 3, ($t > 21.9$ hrs ^{½}), the kinetics of moisture gain is slow, approaching to a plateau corresponding to the equilibrium moisture uptake. The moisture gain curves as a function of time plotted in Fig. 2 shows that all the samples with exception of neat PCL matrix (AR-0) follow a Fickian behavior. These water absorption behaviors are very similar to the results obtained by Cocca et al. [37] with same neat PCL and amorphized cellulose as filler in biocomposite. As expected from the samples that as the aspect ratio increased, the percentage up take of moisture also increased, this was the case for all, apart from aspect ratio of 30 which engrossed the most amount of moisture, having a percentage weight gain of 7.38%.

The remaining samples of aspect ratios of 19, 26 and 38, followed the trend with an increase of 4.29, 5.39 and 5.47%, respectively, over the period of 26.83 hours$^{1/2}$ (744 hours). This is in close agreement with the results obtained when higher content of bamboo fiber was added into nano-hydroxyapatite/poly(lactic-*co*-glycolic), resulted into greater amount of water absorption by the bamboo FRP composite scaffold [33].

3.2. Mechanical properties

3.2.1. Tensile properties

The tensile properties of hemp fiber /PCL composite were evaluated from the data obtained from tensile testing using standard formula. The tensile properties of neat PCL and hemp fiber/PCL biocomposites, such as tensile strength, Young's modulus and extension at break, are presented in Tables 1(a) and (b), respectively.

Apart from aspect ratio of 26, the tensile strength of hemp fiber/PCL biocomposite samples at dry condition does not lead to any improvement in the tensile strength behavior indicating less reinforcing effect. It is well established that the mechanical properties of polymer composites are strongly related to the interfacial strength between fiber and the matrix.

This lack of improvement in tensile strength of hemp fiber/PCL biocomposites with exception of AR 26 may be ascribed to weak interfacial interaction between PCL and hemp fiber. It is well accepted that for lignocellulosic hydrophilic fiber such as hemp to be used efficiently as reinforcing element in a relatively hydrophibic matrix like PCL, the surface of the fiber needs to be compatible by appropriate treatment to reduce its inherent hydrophilic character. Moreover, when natural lignocellulosic fiber reinforced composites are produced by compounding the fibers with matrix materials in extrusion process, one of the main problems arises with the change in fiber length and aspect ratio due to high stresses encountered during the process which significantly influences the

final properties of composites. The main disadvantages of PCL include low modulus and low abrasion resistance. However, with the introduction of hemp into PCL matrix, the stiffness of PCL was enhanced significantly. Evidently, the tensile property (Young's modulus) increases notably from 0.14 GPa to 0.40 GPa (186% improvement) with increasing aspect ratio from neat PCL (AR-0) to 26. This depicts that hemp fiber enhanced the mechanical property of the fiber-reinforced PCL biocomposites. Similar observation on the effect of fibre reinforcement has been reported by Jiang et al. [33]. They concluded that bamboo fiber improved the mechanical properties of nano-hydroxyapatite/poly(lactic-*co*-glycolic) composite scaffold by creating a porous structure. In contrast to tensile strength, the improvement in Young's modulus seems more related to the reinforcing fiber or filler effect, less in the interfacial interaction. From the tensile test results, it can be observed that sample with an aspect ratio of 26 among the hemp fiber/PCL biocomposites showed the highest Young's modulus, which represents an optimal aspect ratio.

More also, it can be observed from Table 1(a) that the extension or elongation at peak load decreases significantly from 12.756 mm (neat PCL matrix) to 4.643 mm for sample with aspect ratio of 26. The extension at peak load for PCL and hemp fiber/PCL biocomposites clearly shows that the introduction of hemp fiber into PCL depicts a significant reduction of elongation at break. These kind of results obtained from neat PCL matrix have been similarly observed and reported on tensile and flexural properties of neat polylactide (PLA), poly(3-hydroxybutyrate-co-hydroxyvalerate) (PHBV), poly(butylene succinate) (PBS) and the tertiary blends [38]. This was generally expected with neat PCL going through the various stages of deformation. Initially, the elastic deformation before strain hardening and necking occurred, as similarly and

earlier reported [38]. The failure of the neat PCL samples was not reached due to its high ductility, but the test provided the critical data needed.

It is considered that for an increase in aspect ratio in saturated samples, the tensile properties decrease due to the relative increase of ingress of moisture in the fibre/matrix interface region. Consequently, it can also be observed from Tables 1(a) and (b) that the tensile modulus is lower for the saturated samples, because the samples have lost some of their stiffness. As far as the structural integrity of tested samples are concerned, tensile strength and tensile modulus have been reduced as a result of saturation. This behavior can be easily attributed to the action of water molecules being able to penetrate into the fiber-matrix interface of wet samples creating a weak fiber-matrix interface resulting poor mechanical performance. Furthermore, the hydrophobic and hydrophilic natures of PCL matrix and hemp fiber, respectively contribute to the difference in their molecular interphase. Therefore, the adhesion between matrix and reinforcement become weaker and resultantly, create an opportunity for increase in water ingression.

3.2.2. Flexural properties

The average flexural properties of dry and water-immersed neat PCL and hemp fiber/PCL composites are similarly presented in Tables 1(a) and (b). It can be observed that all the samples tested show linear behavior initially and then non-linear behavior with the highest maximum load for aspect ratio of 26. Unlike the tensile strength, it can be noticed that hemp reinforced samples have shown significant improvement in flexural strength and modulus. Precisely, the flexural strength increases significantly from 9.53 MPa to 25.6 MPa (169% improvement) with increasing aspect ratio from neat PCL to hemp fiber /PCL of 26. Similarly, the flexural modulus was increased from 0.157 GPa to 0.605 GPa, (285% increase) with increasing aspect ratio from neat to 26.

This improvement is attributed to the effect of reinforcement, which is more noticeable in three-point bending as the loading scenario differs from the tension test. In three point-bending mode, the flexural strength has a combined effect of tensile, compression and shear forces [39].

In addition, there has been a significant loss in the structural rigidity and flexural strength of the water immersed samples. This reduction in flexural properties can be explained further due to the weakening of the fiber-matrix interfacial bond, as a result of water ingress in fibre-matrix interface. An aspect ratio of 26 offers the best flexural properties for both dry and saturated conditions, suggesting that the mechanical performance is significantly enhanced up to a certain aspect ratio, above which the structural rigidity and maximum tolerable force applied decrease.

3.3. Damage characteristics after mechanical (tensile and flexural) tests

With ability to compare the saturated and dry samples side by side is a good visual indication of the differing fracture types. The damage characteristics throughout the samples change greatly between the dry and the water immersed samples. Within the dry samples, the trend of the fracture was cleanly cut through the material, suggesting that the dry samples had a more brittle tendency. The saturated samples however demonstrated a more ductile behavior, as the fracture was not a clean type, instead, the fracture of the water-immersed samples had a rougher edge with greater amount of fiber pull-out, which was visible.

3.4. Low-velocity impact damage response

Fig. 3 depicts the work as a function of time for neat PCL matrix and hemp fiber /PCL biocomposites obtained from low-velocity impact testing. It can be observed that total energy absorbed by the neat PCL sample is greater than all other hemp fiber/PCL samples in both conditions. Sample AR-0 performs differently, this show how the work

is distributed around the sample. Comparatively, sample AR-38 absorbs greatest energy among other reinforced samples at dry condition immediately after 10 ms, while sample AR-26 absorbed the lowest (Fig. 3(a)). However, sample AR-38 absorbed the lowest (reduced) energy at wet condition and sample AR-19 exhibits little energy reduction, while other samples (AR-0, 26 and 30) exhibit increased values. This increase is much with sample AR-26, as shown in Fig. 3(b), having the best impact resistance from dry to wet conditions, among others.

The result in moisture absorption aided the impact response, thus resulting in greater energy required to puncture the samples. Sample AR-30 did not show a significant response to the effect of moisture within the samples, it however increased slightly in the energy absorbed, but only by 0.8 J. This increase is expected from a saturated natural fiber composite. With sample AR-38, the influence of moisture within the sample caused the total amount of work required before the drop weight punctured fell from nearly 28 J down to approximately 20 J, showing a large loss in energy of around 8 J. After saturation (Fig. 3(b)), the structural integrity of all samples maximum force amount of energy absorbed by AR-19 reduced from 25 J to around 21 J. AR-26 sample exhibited properties of a natural fiber composite, as shown with an increase in energy absorbed from 18 J in its dry state to 22 J once saturated.

Furthermore, the energy absorbed by each sample changes with the aspect ratio, with a range from 18 J to 28 J. When the samples are saturated, there is an increase in the amount of energy required to puncture the samples. By comparing the two results, it is evident that the saturated samples exhibit a shallower gradient before reaching the maximum work. The saturated samples on average follow the trend that a larger force is required to puncture the samples. Considering the sample of AR-26, from the impact

response data, it is observed that under saturated conditions, it performs better in comparison to other composites with different aspect ratios. The saturated samples absorb more energy than the dry samples, which increase by nearly 4 J, from 18 J to 22 J with dry to saturated samples, respectively. This scenario is attributed to the weak fibre-matrix interfaces at the wet conditions allowing dissipation of more energy within the interfaces.

Figs 4(a) and (b) depict how the hemispherical impact tup bounced off the sample with sample AR-0 soon after impact for both dry and wet conditions respectively, indicating that it had a good elasticity, being able to rebound the drop weight without puncture. This is similar to the saturated samples, but with higher deflection (standard travel) as the moisture seems to dampen the elasticity and absorbs more energy. The trend for the dry hemp fiber/PCL composites shows that at around 5 ms after initial contact with the hemispherical impactor, maximum force has been achieved with the samples before they began to fracture and later penetrated, as shown in Figs 4(c) and (d). Among these HF/PCL samples, sample of aspect ratio of 19 has the greatest impact force of 2639 N at dry condition. This is possible due to the presence of PCL matrix, being able to have a greater effect on the impact damage performance compared to other HF/PCL biocomposite samples. Similarly, sample with aspect ratio of 26 has the lowest impact force of 1813 N at dry condition. Evidently, there is a clear difference between how the aspect ratio alters the total force required to puncture the FRP composite samples. In terms of force versus time, as depicted in Figs 4(c) and (d), with saturated condition, from force of 1813 N for the dry sample before puncture to a force of nearly 2000 N for the saturated samples. This increase in the amount of force required to penetrate the sample is only recorded in the sample AR-0, while there is decrease in the force across other samples at wet condition.

3.5. Damage characteristics after low-velocity impact

From visual inspection, there is a clear difference between the dry and saturated samples throughout the aspect ratios. The water-immersed samples have fared better damage by withstanding the impactor and failed to puncture through the majority of the samples. This however cannot be said of the dry samples as many of them were fully penetrated. This was clearly observed by visual comparison of samples of AR-19 and AR-26. It has been reported that the nano-fiber-reinforced polystyrene (PS) has a greater mechanical performance when compared to unreinforced PS materials [3]. Similar to the enhancement of mechanical strength of a grafted hydroxyapatite/PCL composite tablets as possible substitutes for bone, due to an improved cell division [40].

3.6. Scanning electron microscopy

A scanning electron microscope was used to examine the micrographs of the impacted areas on the different aspect ratio samples. Four magnifications of the micrographic images were taken: 50, 150, 300 and 500 x, each is able to show a different level of the damaged area, clearly with 300 x as representative magnification.

The collation of SEM images in Fig. 5 compares the selected micrographs of the four HF/PCL samples of different aspect ratios and conditions, it is evident that the number of crazes present increased from aspect ratio of 19 to 38. These increased crazes were also observed between the saturated and the dry samples, whereby the saturated samples have a greater number of crazes than the dry samples. The increased fibrillation within the saturated samples makes the PCL matrix to deform more, enabling the transfer of stress through the composite.

3.7. X-ray micro computed tomography

The micrographs of the optimum sample of AR-26 was examined under X-ray μCT. It is evident that both radial and circumferential fractures were present in the impacted

sample (Figs 6(a) and (b)), which reduced with an increase in aspect ratio of other HF/PCL samples.

Additionally, there was a ductile fracture which was indicated by the irregular and rough pattern of cut on the fractured surfaces of the samples, as depicted in Fig. 6(c). However, the ductile nature of the HF/PCL samples was reduced with more rough and irregular fractures as aspect ratio increased. Mostly, cleaner, straight/linear or perpendicular pattern of fracture on the surfaces of damaged materials are characterized by brittle fractures.

4. Conclusions

This paper has investigated the effects of aspect ratio and water absorption on the mechanical performances of hemp fiber/polycaprolactone biocomposites. The results showed evidence that with an increase in aspect ratio, the rate and quantity of moisture uptake was increased. With exception of neat PCL, all other samples followed Fick's law of diffusion with an increase in diffusion coefficient as the aspect ratio increased. Samples with aspect ratios 19, 26, 30 and 38 increased in weight by 4.29, 5.39, 7.38 and 5.54%, respectively.

The effect of moisture ingress in the samples dramatically reduced the tensile and flexural modulus. Based on the observation of the SEM micrographs obtained from the impacted samples, delamination at the interface and fiber pull-out seemed to be more rampant within the saturated samples, while the X-ray µCT depicted circumferential and radial fractures at the front and rear parts of the HF/PCL biocomposite samples, implying irregular and rough pattern (ductile) fractures.

Based on all the experimental tests performed, a trend was observed that suggests that there is a threshold value for the hemp fiber aspect ratio, which was 26. Hence,

HF/PCL biocomposite sample of the aspect ratio of 26 outperformed the other samples in both dry and saturated conditions.

Funding: None of the authors has received funds for the study reported here.

References

[1] D. Trachea, M. H. Hussinb, M. K. M. Haafizc, V. K. Thakur, Recent progress in cellulose nanocrystals: sources and production, Nanoscale, 9 (2017) 1763- 1786.

[2] A. Arbelaiz, B. Ferna´ndez, A. Valea, I, Mondragon, Mechanical properties of short flax fiber bundle/poly (3-caprolactone) composites: Influence of matrix modification and fiber content, Carbohydr. Polym. 64 (2006) 224-232.

[3] D. Ballner, S. Herzele, J. Keckes, M. Edler, T. Griesser, B. Saake, F. Liebner, A. Potthast, C. Paulik, W. Gindl-Altmutter, Lignocellulose nanofiber-reinforced polystyrene produced from composite microspheres obtained in suspension polymerization shows superior mechanical performance, ACS Appl. Mat. Interf. 8 (2016) 13520 − 13525.

[4] H.N. Dhakal, Z.Y. Zhang, M.O.W. Richardson, Effect of water absorption on the mechanical properties of hemp fiber reinforced unsaturated polyester composites, Compos. Sci. Technol. 67 (2007) 1674-1683.

[5] M. Jawaid, H.P.S. Abdul Khalil, Cellulosic/synthetic fibre reinforced polymer hybrid composites: A review, Carbohydr. Polym. 86 (2011) 1-18.

[6] K. Joseph, S. Thomas, Effect of chemical treatment on the tensile properties of short sisal fibre-reinforced polyethylene composites, Polym. 37 (1996) 5139-5149.

[7] M.A. Khan, M.M. Hassan, L.T. Drzal, Effect of 2-hydroxyethyl methacrylate (HEMA) on the mechanical and thermal properties of jute-polycarbonate composite, Compos. Part A Appl. Sci. Manuf. 36 (2005) 71-81.

[8] L. Ludue˜na, A. Vázquez, V. Alvarez, Effect of lignocellulosic filler type and content on the behavior of polycaprolactone based eco-composites for packaging applications, Carbohydr. Polym. 87 (2012) 411-421.

[9] M.O.W. Richardson, T.J. Santana, J. Hague, Natural fibre composites-the potential for the Asian markets, Prog. Rubb. Plast.Technol. 14 (1998) 174-188.

[10] A.K. Bledzki, J. Gassan, Composites reinforced with cellulose based fibres, Prog. Polym. Sci. 24 (1998) 221-274.

[11] A. Bourmaud, H. Dhakal, A. Habrant, J. Padovani, D. Siniscalco, M.H. Ramage, J. Beaugrand, D.U. Shah, Exploring the potential of waste leaf sheath date palm fibres for composite reinforcement through a structural and mechanical analysis, Compos. Part A Appl. Sci. Manuf, 103 (2017) 292 –303.

[12] A.K. Mohanty, M. Misra, L.T. Drzal, Sustainable biocomposites from renewable resources: Opportunities and challenges in the green materials world, J. Polym. Environ. 10 (2002) 19-26.

[13] S.P. Dubey, V.K. Thakur, S. Krishnaswamy, H.A. Abhyankar, V. Marchante, J. L. Brighton, Progress in environmental-friendly polymer nanocomposite material from PLA: Synthesis, processing and applications, Vacuum, 146 (2017) 655- 663.

[14] A.C. Wibowo, A.K. Mohanty, M. Misra, L.T. Drzal, Chopped industrial hemp fiber reinforced cellulosic plastic biocomposites: thermomechanical and morphological properties, Ind. Eng. Chem. Res. Mat. Interf. 43 (2004) 4883 − 4888.

[15] H.N. Dhakal, V. Skrifvars, K. Adekunle, Z.Y. Zhang, Falling weight impact response of jute/methacrylated soybean oil bio-composites under low-velocity impact loading, Compos. Sci. Technol. 92 (2014) 134 -141.

[16] O. Faruk, A.K. Bledzki, H.P. Fink, M. Sain, Biocomposites reinforced with natural fibres: 2000-2010, Prog. Polym. Sci. 37 (2012) 1552-1596.

[17] M.A. Khan, J. Ganster, H.P. Fink, Hybrid composites of jute and man-made cellulose fibres with polypropylene by injection moulding, Compos. Part A Appl. Sci. Manuf. 40 (2009) 846-851.

[18] L.Y. Mwaikambo, M.P. Ansell, Chemical modification of hemp, sisal, jute and kapok fibres by alkalization, J Appl. Polym. Sci. 84 (2002) 2222-2234.

[19] V.K. Thakur, D. Vennerberg, M.R. Kessler, Green aqueous surface modification of polypropylene for novel polymer nanocomposites, ACS Appl. Mat. Interf. 6 (2014) 9349 − 9356.

[20] H.N. Dhakal, Z.Y. Zhang, R. Guthrie, J. MacMullen, N. Bennett, Development of flax/carbon fibre hybrid composites for enhanced properties, Carbohydr. Polym. 96 (2013) 1-8.

[21] Directive. (2000). 2000/53/EC of the European parliament and the council for end-of-life vehicles, official journal of the European communities, Oct 21, 2000, ABl.EG Nr. L 269 S. 34L 269/34

[22] S. Farah, D.G. Anderson, R. Langer, Physical and mechanical properties of PLA, and their functions in widespread applications - A comprehensive review, Adv. Drug Deliv. Rev. 107 (2016) 367 – 392.

[23] M. Murariu, P. Dubois, PLA composites: From production to properties, Adv. Drug Deliv. Rev. 107 (2016) 17 – 46.

[24] P. Dhar, A. Kumar, V. Katiyar, Magnetic cellulose nanocrystal based anisotropic polylactic acid nanocomposite films: Influence on electrical, magnetic, thermal, and mechanical properties, ACS Appl. Mat. Interf. 8 (2016) 18393 − 18409.

[25] V. Arias, J. Odent, J. Raquez, P. Dubois, K. Odelius, A. Albertsson, Toward “green” hybrid materials: Core-shell particles with enhanced impact energy absorbing ability, ACS Sustain. Chem. Eng. 4 (2016) 3757−3765.

[26] A. Pappua, V. Patil, S. Jain, A. Mahindrakar, R. Haquea, V. K. Thakur, Advances in industrial prospective of cellulosic macromolecules enriched banana biofibre resources: A review, Int. J. Biol. Macromol. 79 (2015) 449–458.

[27] A.S.F. Talla, F. Erchiqui, F. Godard, D. Kocaefe, An evaluation of the thermal degradation kinetics of novel melt processed PET-Hemp fiber composites, J. Therm. Anal. Calorim. 126 (2016) 1387-1396.

[28] M. Tazi, F. Erchiqui, H. Kaddami, Influence of softwood-fillers content on the biodegradability and morphological properties of wood-polyethylene composites, Polym. Compos. 39 (2018) 29-37.

[29] A. Bravo, L. Toubal, D. Koffi, F. Erchiqui, Damage characterization of bio and green polyethylene–birch composites under creep and cyclic testing with multivariable acoustic emissions, Materials, 8 (2015) 7322-7341.

[30] A. Bravo, L. Toubal, D. Koffi, F. Erchiqui, Development of novel green and bio composite materials: Tensile and flexural properties and damaging analysis using acoustic emission. Mater. Des. 66 (2015) 16-28.

[31] A.S.F. Talla, E. Mfoumou, S. Jeson, J.S.Y.D. Page´, F. Erchiqui, Mechanical and structural properties of a novel melt processed PET-hemp composite: Influence of additives and fibers concentration, J. Reinf. Plast. Compos. 32 (2013) 1526-1533.

[32] A.S.F. Talla, F. Erchiqui, H. Kaddami, D. Kocaefe, Investigation of the thermostability of PET-hemp fiber composites: Extending natural fiber reinforcement to high-melting thermoplastics, J. Appl. Polym. Sci. 132 (2015) 1-10.

[33] L. Jiang, Y. Li, C. Xiong, S. Su, H. Ding, Preparation and properties of bamboo fiber/nano-hydroxyapatite/poly(lactic-co-glycolic) composite scaffold for bone tissue engineering, ACS Appl. Mat. Interf. 9 (2017) 4890 − 4897.

[34] T. Wang, L.T. Drzal, Cellulose-nanofiber-reinforced poly-(lactic acid) composites prepared by a water-based approach, ACS Appl. Mat. Interf. 4 (2012) 5079 − 5085.

[35] J. Beaugrand, F. Berzin, Lignocellulosic fiber reinforced composites: influence of compounding conditions on defibrization and mechanical properties, J. Appl. Polym. Sci. 128 (2013) 1227-1238.

[36] Determination of puncture impact behaviour of rigid plastics. British standard, Part 2: instrumented puncture testing. BS EN ISO 6603–2; 2000.

[37] M. Cocca, R. Avolio, G. Gentile, E. Di Pace, M.E. Errico, M. Avella, Amorphized cellulose as filler in biocomposites based on poly(Ɛ-caprolactone), Carbohydr. Polym. 118 (2015) 170 -182.

[38] K. Zhang, A.K. Mohanty, M. Misra, Fully biodegradable and biorenewable ternary blends from polylactide, poly(3-hydroxybutyrate-co-hydroxyvalerate) and poly(butylene succinate) with balanced properties, ACS Appl. Mat. Interf. 4 (2012) 3091 − 3101.

[39] S. Das, Mechanical properties of waste paper/jute fabric reinforced polyesterresin matrix hybrid composites, Carbohydr. Polym. 172 (2017) 60 - 67.

[40] D.W. Hong, Z.T. Lai, T.S. Fu, T.T. Tsai, I.M. Chu, P.L. Lai, The influences of polycaprolactone-grafted nanoparticles on the properties of polycaprolactone composites with enhanced osteoconductivity, Compos. Sci. Technol. 83 (2013) 64 - 71.

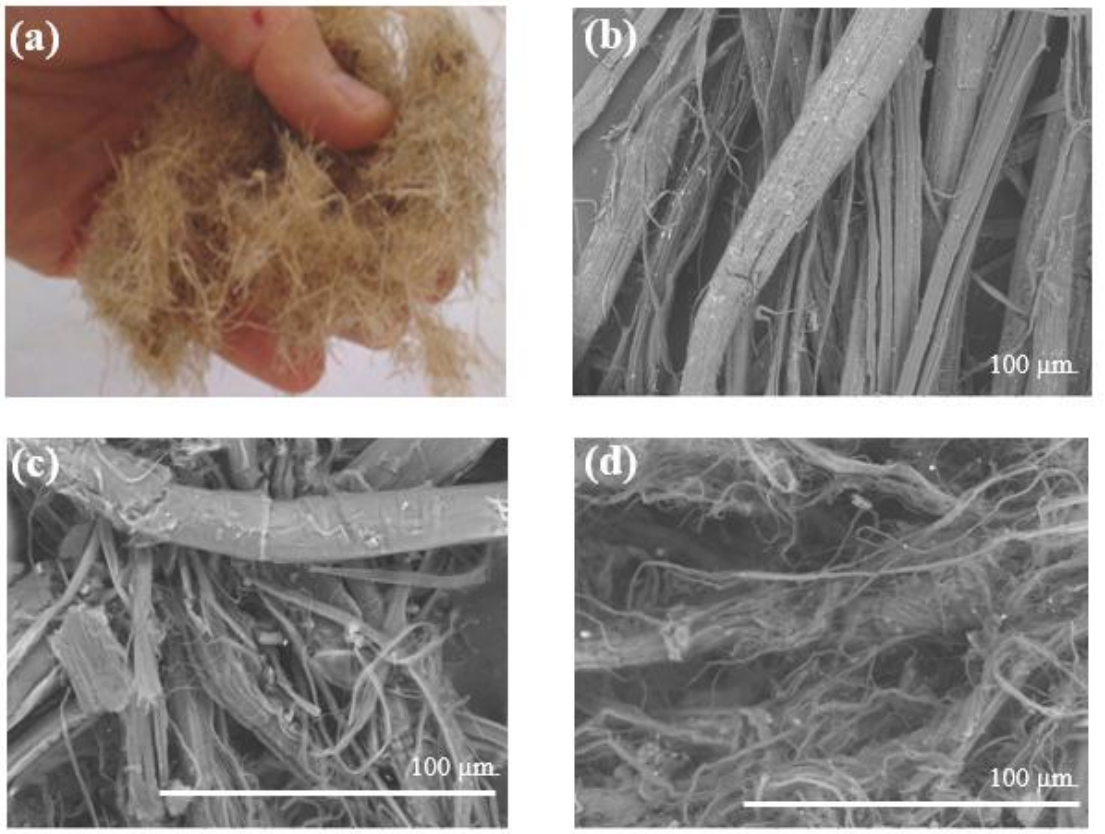

Fig. 1. Micrographs representative of the fiber populations. In (a) the raw hemp fiber fraction, where very large bundles (millimetric) are visible. In (b), (c) and (d) are scanning electron microscope views of the fiber populations.

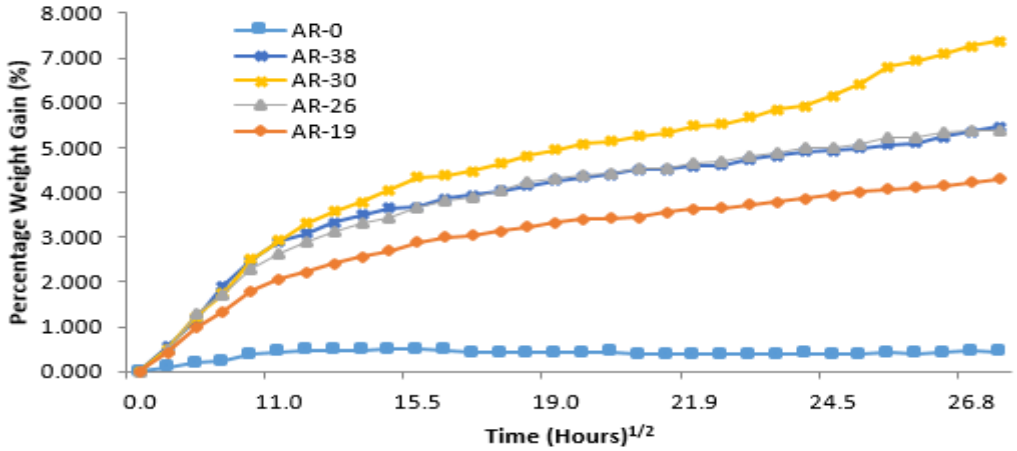

Fig. 2. Water absorption behavior of PCL matrix (AR-0) and hemp fiber /PCL biocomposite samples with different aspect ratios.

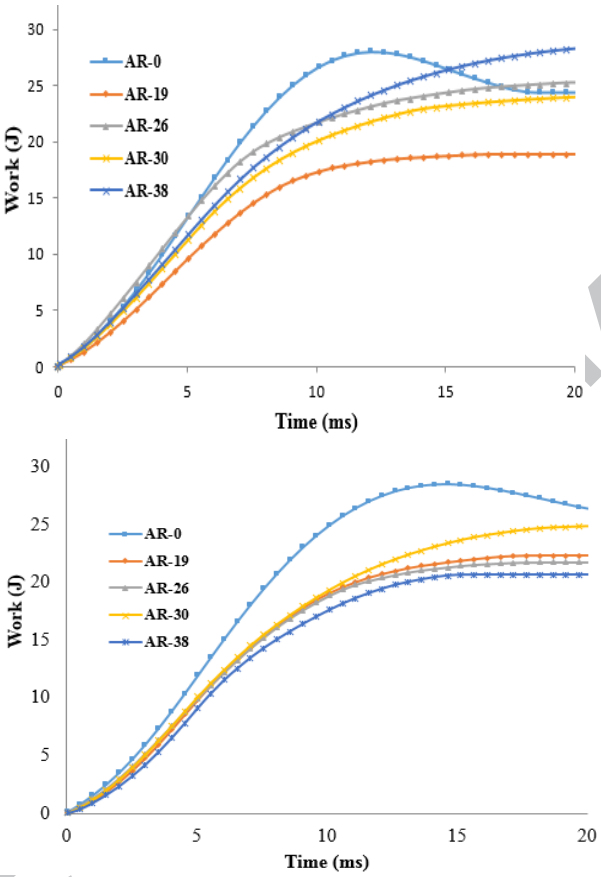

(a) **(b)**

Fig. 3. Work versus time curves for (a) dry and (b) water-immersed samples, showing distinctive performance of both dry and wet neat PCL matrix (AR-0) and other samples.

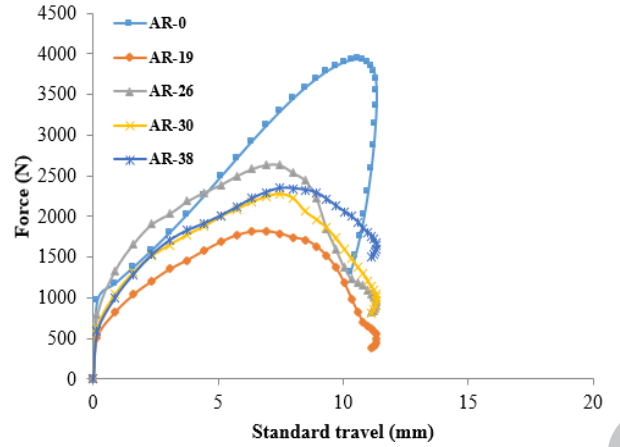

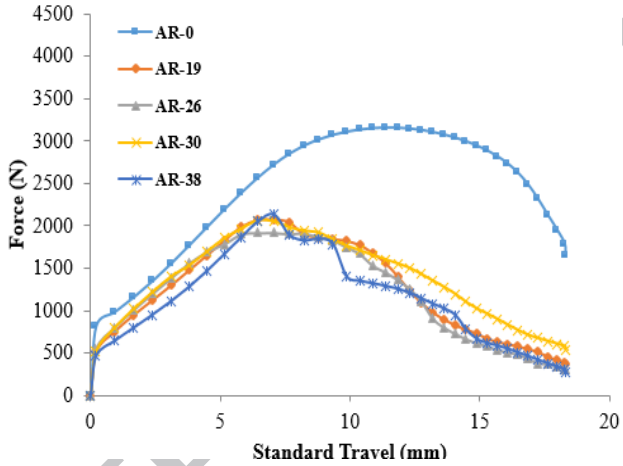

(a) (b)

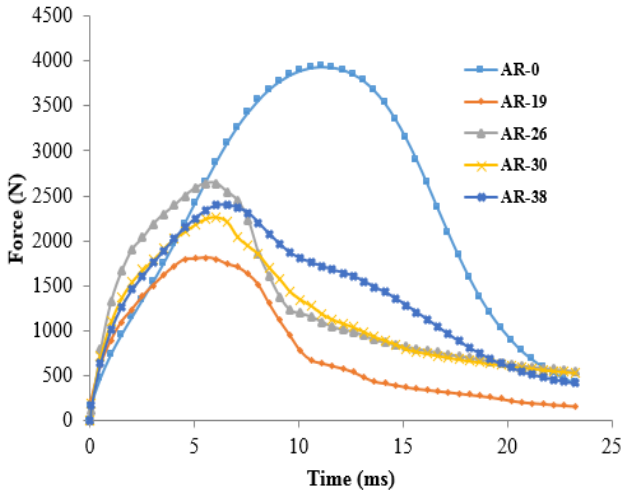

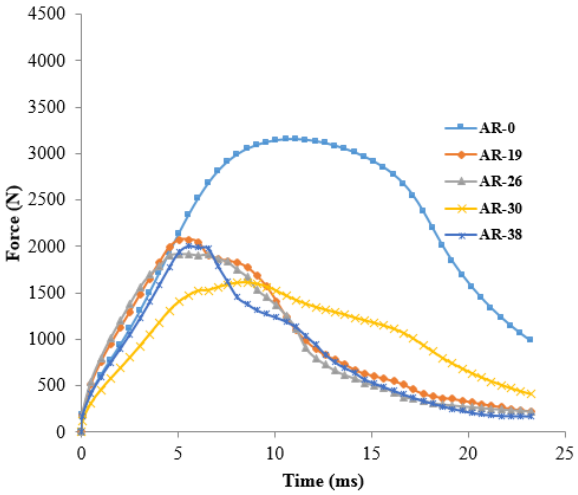

(c) (d)

Fig. 4. Force versus standard travel curves for (a) dry and (b) water-immersed samples, depicting the rebounding phenomenon of the drop weight/impactor head without puncture, and force versus time curves (c) dry and (d) water-immersed samples, showing outstanding elastic behavior of both dry and wet neat PCL matrix samples (AR-0).

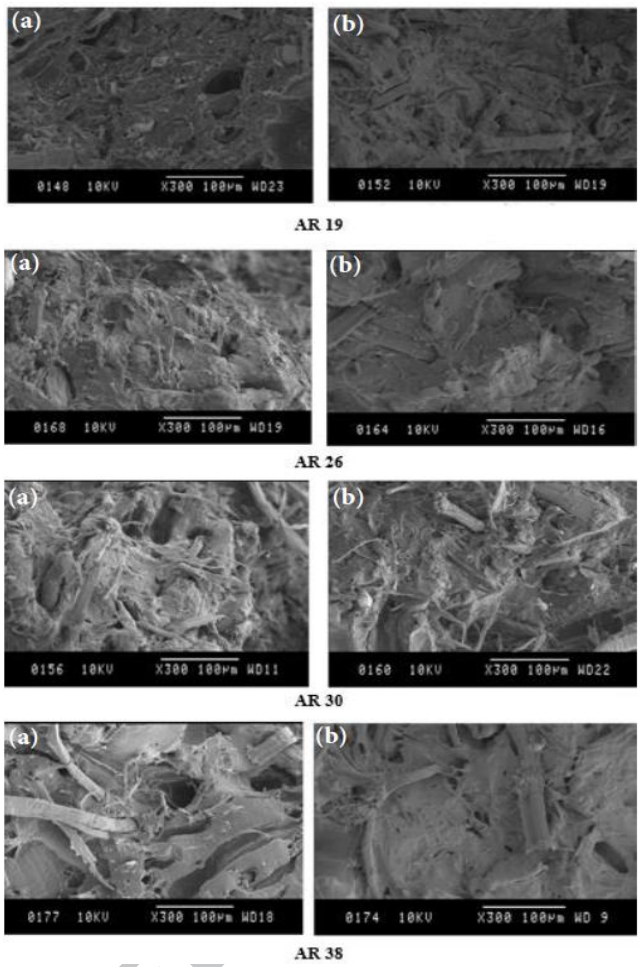

Fig. 5. SEM micrographs of fractured samples under impact testing at (a) dry and (b) wet.

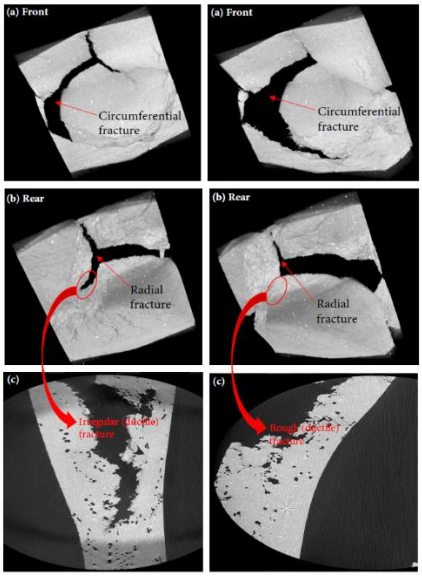

Fig. 6. X-ray µCT micrographs of HF/PCL optimum impacted dry sample of AR-26, showing (a) circumferential fractures at the front parts, (b) radial fractures at the rear

parts of the sample, while (c) depicting irregular and rough pattern (ductile) fractures on the surfaces.

Table 1(a): Tensile and flexural properties of different samples at dry condition.

Samples	Tensile strength (MPa)	Tensile modulus (GPa)	Elongation at break (mm)	Flexural strength (MPa)	Flexural modulus (GPa)	Deformation at peak load (mm)
Neat PCL	11.73 (±0.10)	0.14 (±0.001)	12.756 (±0.10)	9.53 (±0.13)	0.157 (±0.002)	18.73 (±0.21)
AR 19	10.02 (±0.42)	0.27 (±0.012)	5.52 (±0.26)	14.9 (±0.24)	0.317 (±0.006)	16.19 (±0.22)
AR 26	12.25 (±0.52)	0.40 (±0.021)	4.643 (±0.35)	25.68 (±0.26)	0.605 (±0.006)	14.16 (±0.18)
AR 30	11.97 (±0.21)	0.36 (±0.017)	4.898 (±0.19)	23.72 (±0.39)	0.325 (±0.009)	15.09 (±0.73)
AR 38	11.77 (±0.18)	0.27 (±0.007)	6.555 (±0.14)	16.94 (±0.22)	0.364 (±0.006)	15.73 (±0.27)

Table 1(b): Tensile and flexural properties of different samples at water-immersed condition.

Samples	Tensile strength (MPa)	Tensile modulus (GPa)	Elongation at break (mm)	Flexural strength (MPa)	Flexural modulus (GPa)	Deformation at peak (mm)
Neat PCL	13.36 (±0.34)	0.17 (±0.006)	12.130 (±0.11)	13.41 (±0.94)	0.218 (±0.019)	19.158 (±0.52)
AR 19	8.63 (±0.02)	0.17 (±0.012)	7.834 (±0.54)	11.11 (±0.46)	0.220 (±0.006)	17.144 (±0.23)
AR 26	12.21 (±0.49)	0.21 (±0.01)	8.696 (±0.84)	18.29 (±0.81)	0.374 (±0.028)	17.912 (±0.62)
AR 30	9.60 (±0.42)	0.164 (±0.014)	8.741 (±0.86)	13.67 (±0.28)	0.274 (±0.008)	16.692 (±0.29)
AR 38	9.78 (±0.32)	0.17 (±0.016)	8.520 (±0.89)	14.35 (±0.11)	0.281 (±0.005)	17.424 (±0.60)